

Supplementary Materials

SARS-CoV-2 structure and replication characterized by in situ cryo-electron tomography

Steffen Klein[#], Mirko Cortese[#], Sophie L. Winter[#], Moritz Wachsmuth-Melm, Christopher J. Neufeldt, Berati Cerikan, Megan L. Stanifer, Steeve Boulant, Ralf Bartenschlager^{*}, Petr Chlanda^{*}

^{*} Correspondence to: petr.chlanda@bioquant.uni-heidelberg.de,
ralf.bartenschlager@med.uni-heidelberg.de

[#] Equal contribution

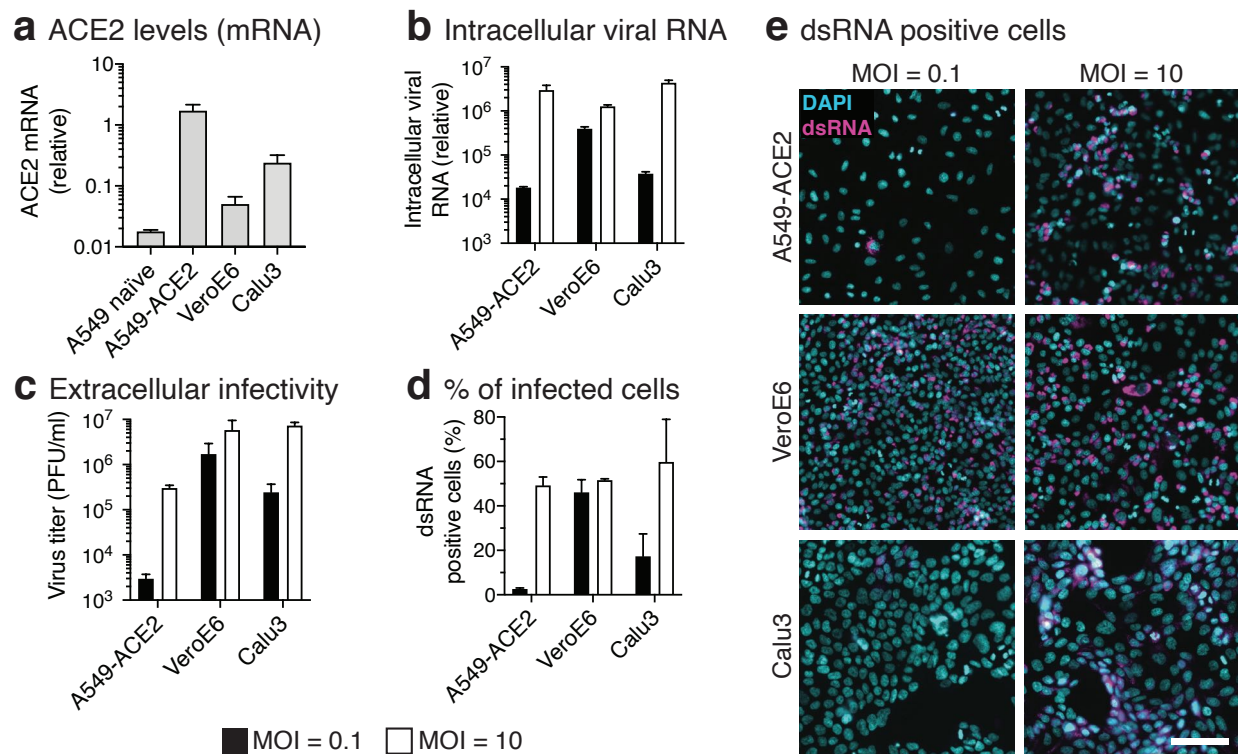


Figure S1 | ACE2 mRNA levels and SARS-CoV-2 infection in A549-ACE2, VeroE6 and Calu3 cells. All experiments were performed in triplicates. Data are shown as a bar plot with indicated standard deviation. **a**, ACE2 mRNA levels normalized to HPRT mRNA levels of the three cell lines used in this study determined by RT-qPCR. **b**, Intracellular viral RNA levels (normalized to HPRT mRNA) of the three cell lines infected with SARS-CoV-2 at 16hpi with MOI 0.1 (black) or 10 (white) determined by RT-qPCR. **c**, Released extracellular virus measured as plaque forming units (PFU) per ml for the three cell lines infected with SARS-CoV-2 at 16hpi with MOI 0.1 (black) or 10 (white). **d**, Percentages of dsRNA positive cells for the three cell lines infected with SARS-CoV-2 at 16 hpi with MOI 0.1 (black) or 10 (white). **e**, Wide-field fluorescent light microscopy images used for analysis in (d) showing DAPI stained cell nuclei (cyan) and staining with an anti-dsRNA antibody (magenta) in the three cell lines infected with SARS-CoV-2 16 hpi with MOI 0.1 and 10. Scale bar: 100 µm.

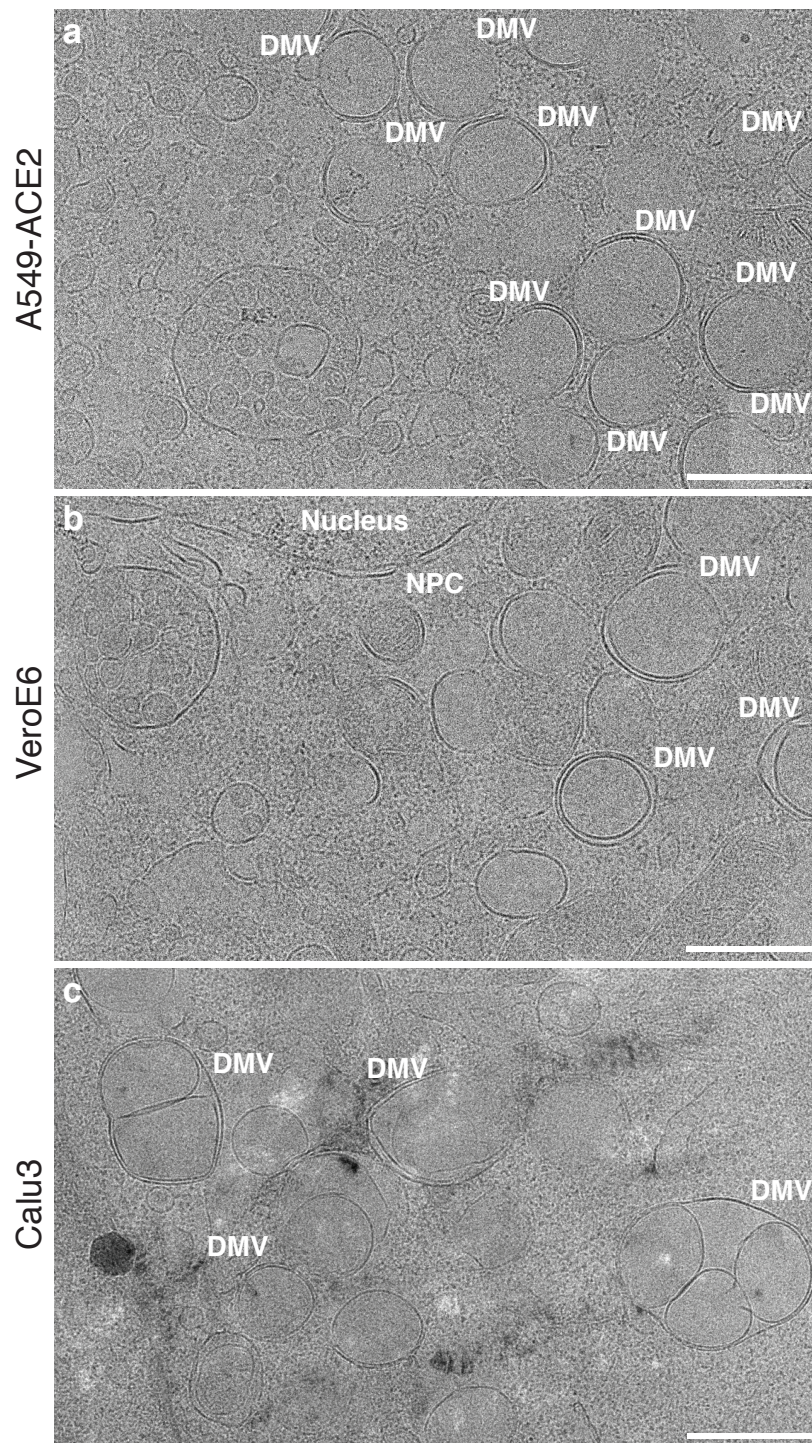


Figure S2 | Cryo-EM of DMVs in A549-ACE2, VeroE6 and Calu3 cells. Exemplary images from cryo-EM montages on milled A549-ACE2 (a), VeroE6 (b) and Calu3 (c) cells that were used for tomogram acquisition of DMVs and fused DMVs in Calu3 cells. Due to the thickness of Calu3 and increased clustering of cells, Calu3 cryo-lamellae samples showed partially vitrified regions more frequently. Scale bars: (a–c) 500 nm.

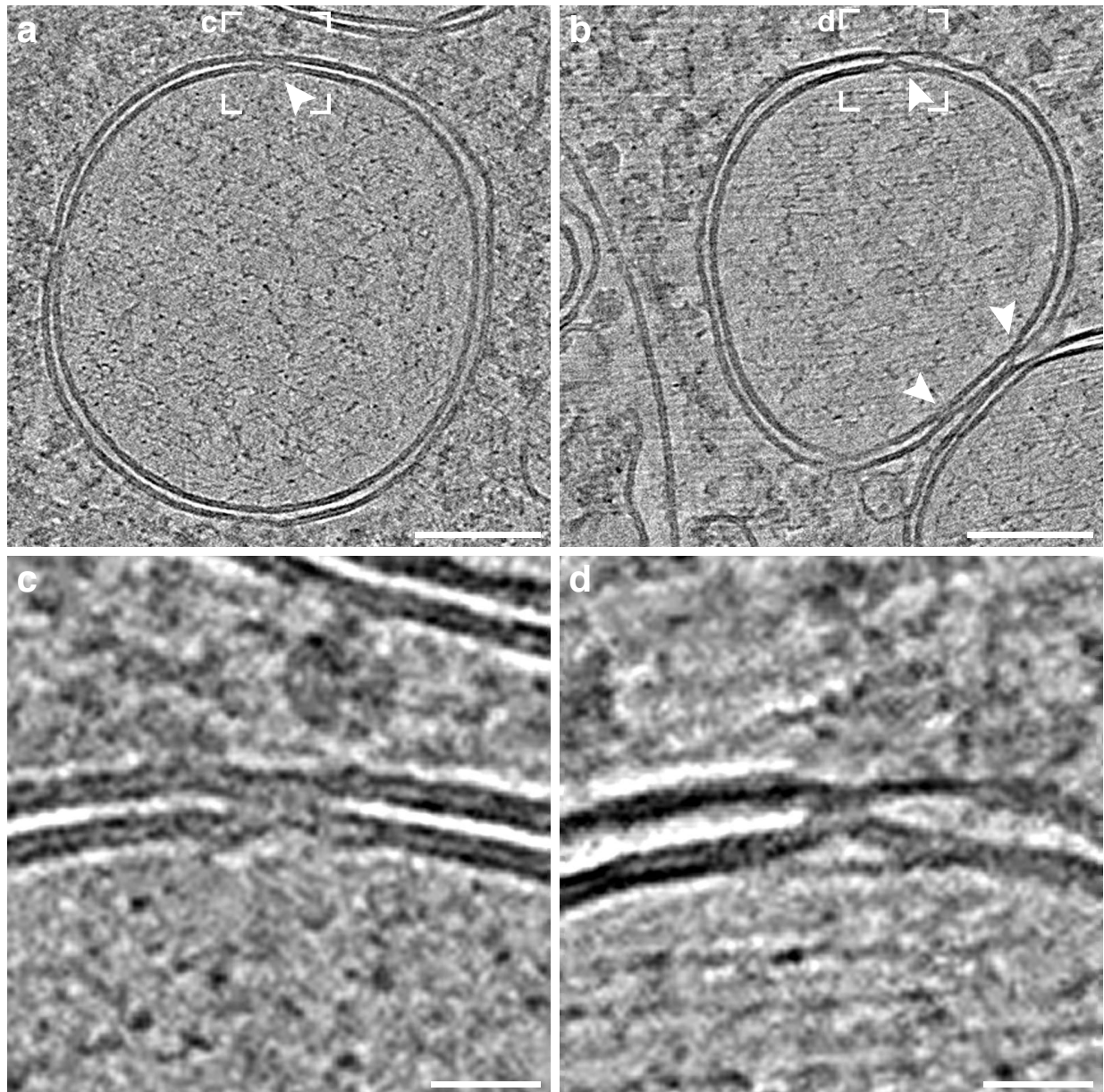


Figure S3 | Putative pore complexes clamping the inner and outer DMV membrane and connecting the DMV lumen with the cytoplasm. a, b Slices of tomograms showing DMVs with sites of putative pores (arrowheads), spanning both membranes of the DMV. **c, d**, Magnified images of the putative pore complex. Scale bars: (a, b) 100 nm, (c, d) 20nm

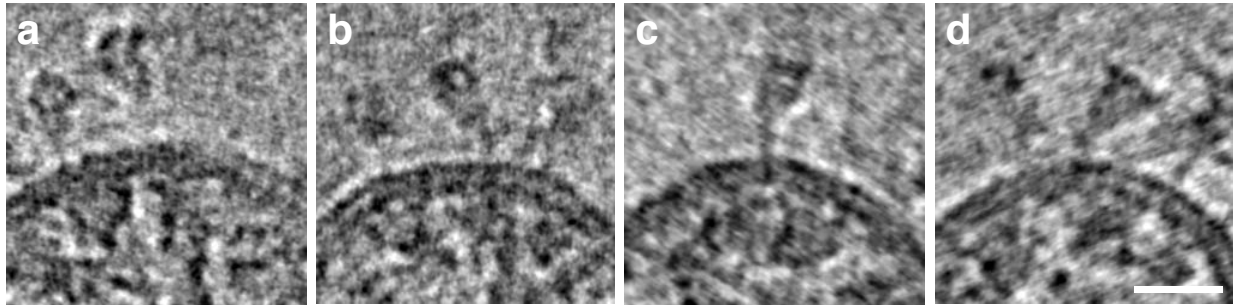


Figure S4 | Tilted spike glycoproteins of intracellular virions. Slices of tomograms showing individual S trimers with different tilting angles relative to the viral envelope of 31° (a), 35° (b), 37° (c) and 41° (d). 20 tomogram slices were average and low pass filtered (2 pixel). Scale bar: 20 nm.

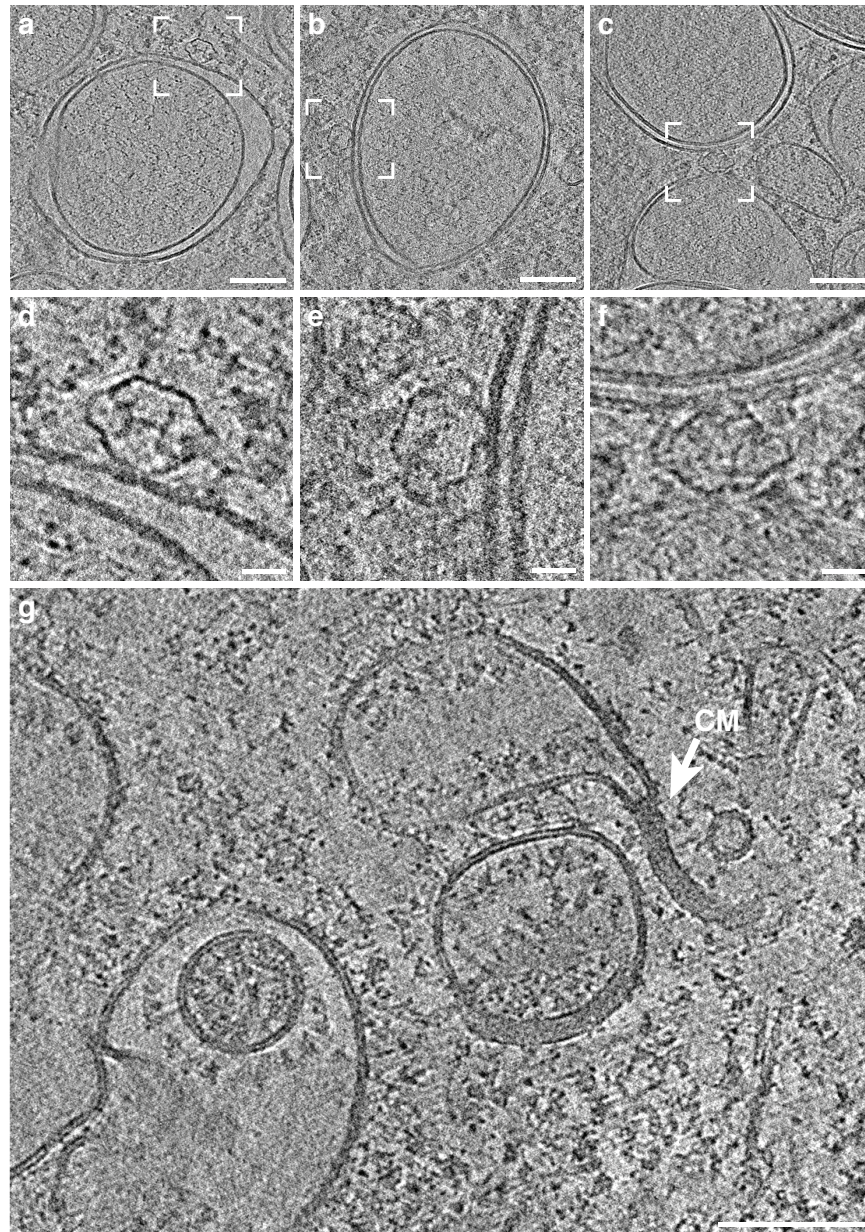


Figure S5 | Vault protein complex in the proximity of DMV and putative convoluted membrane. **a–f**, Slices of tomograms (average of 10 slices) showing 3 examples of vault complexes in the proximity of the DMV outer membrane found in SARS-CoV-2 infected VeroE6 (a, c, d, f) and in A549-ACE2 cells (b, e). vault complexes are oriented with the longitudinal axis along the outer membrane in all observed cases. In one case a vault complex was found to be located between two DMVs (c, f). **g**, Slice of a tomogram of SARS-CoV-2 infected Calu3 cell showing a putative zippered ER cisterna (CM; convoluted membrane) characteristic of a density found inside the cisternae. The diameter of the CM is approximately 18 nm. Scale bars: (a, b, c, d, g) 100 nm, (d, e, f) 20 nm.

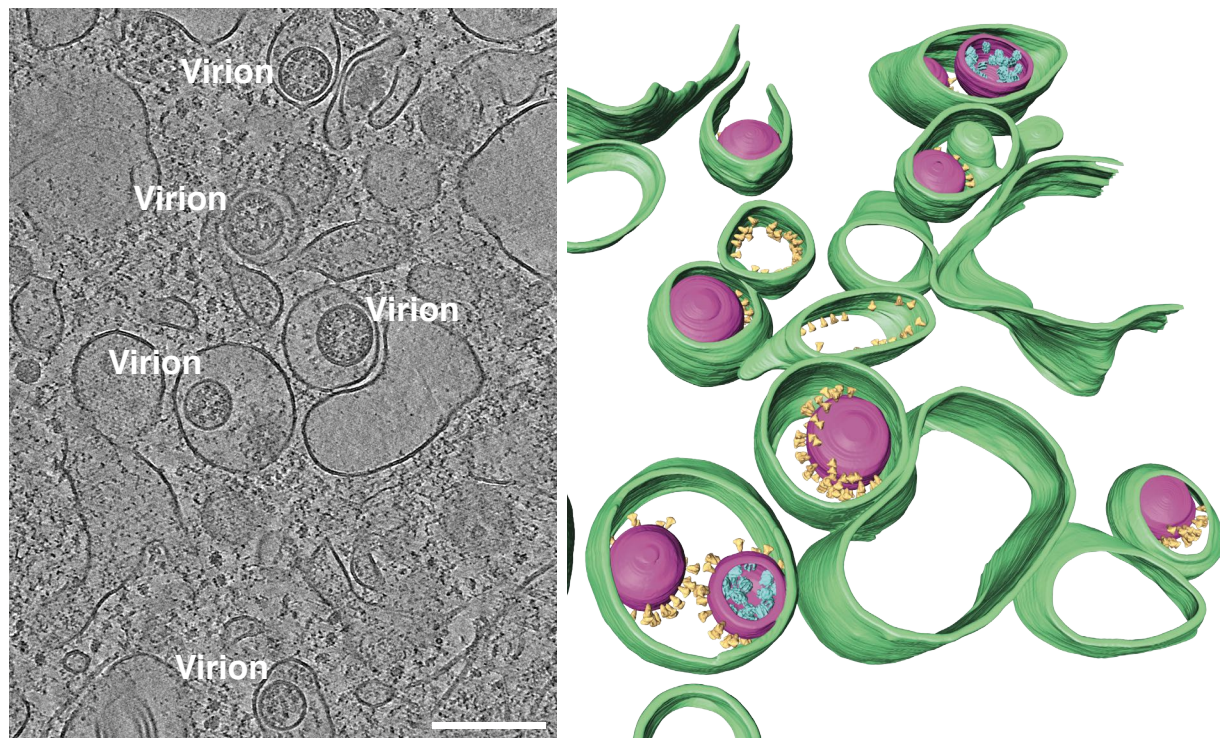


Figure S6 | Assembled intracellular virions. Tomogram showing a VeroE6 cell infected with SARS-CoV-2 at 16hpi. 20 slices of the tomogram were averaged, and a non-local means filter was applied. Intracellular released virions inside the ERGIC lumen are indicated. A 3D volume rendering is shown with cellular membranes (green) and viral membranes (magenta). For each S glycoprotein (yellow) and vRNP (cyan) present in the tomogram the subtomogram average of S glycoprotein was placed in the volume rendering. The S trimer average orientations represent the data in the tomogram, whereas the vRNP average orientations were randomized (Movie S3). Scale bar: 200 nm.

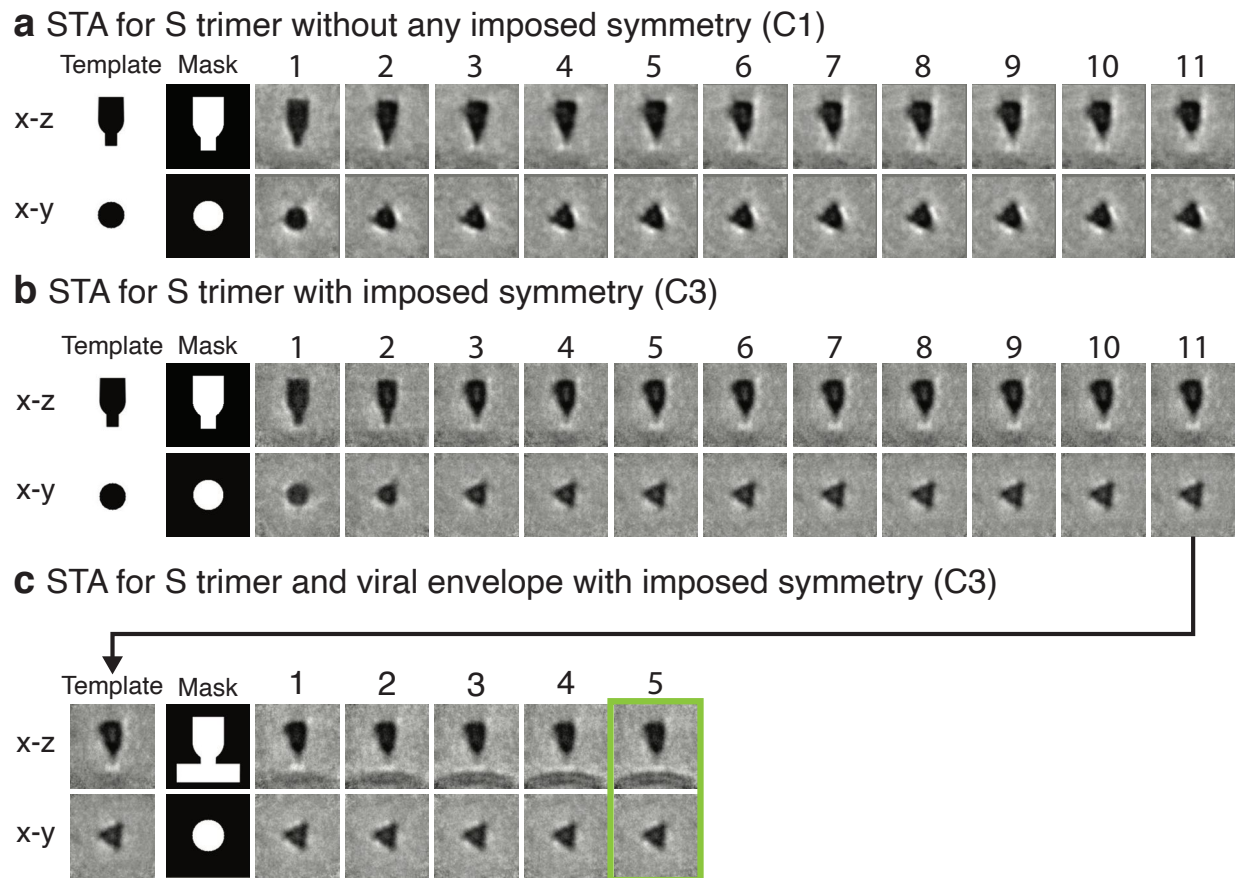


Figure S7 | Overview of S trimer subtomogram averaging. Particles ($n = 219$) corresponding to positions of S trimers in tomograms acquired on cryo-lamella of SARS-CoV-2 infected VeroE6 cells were cropped ($160 \times 160 \times 160$ voxels) in Dynamo using the 'general' model. **a**, Particles were iteratively aligned and averaged using a template and mask shown on the left without imposing any symmetry. **b**, Particles were iteratively aligned and averaged using a template and mask shown on the left with c3 symmetry imposed. **c**, Particles were iteratively aligned and averaged using the final average obtained in (b) as a template and a mask shown on the left with c3 symmetry imposed. The final average in B and the final average (green) were c3-symmetrized and used for model fitting in ChimeraX (Movie S4).

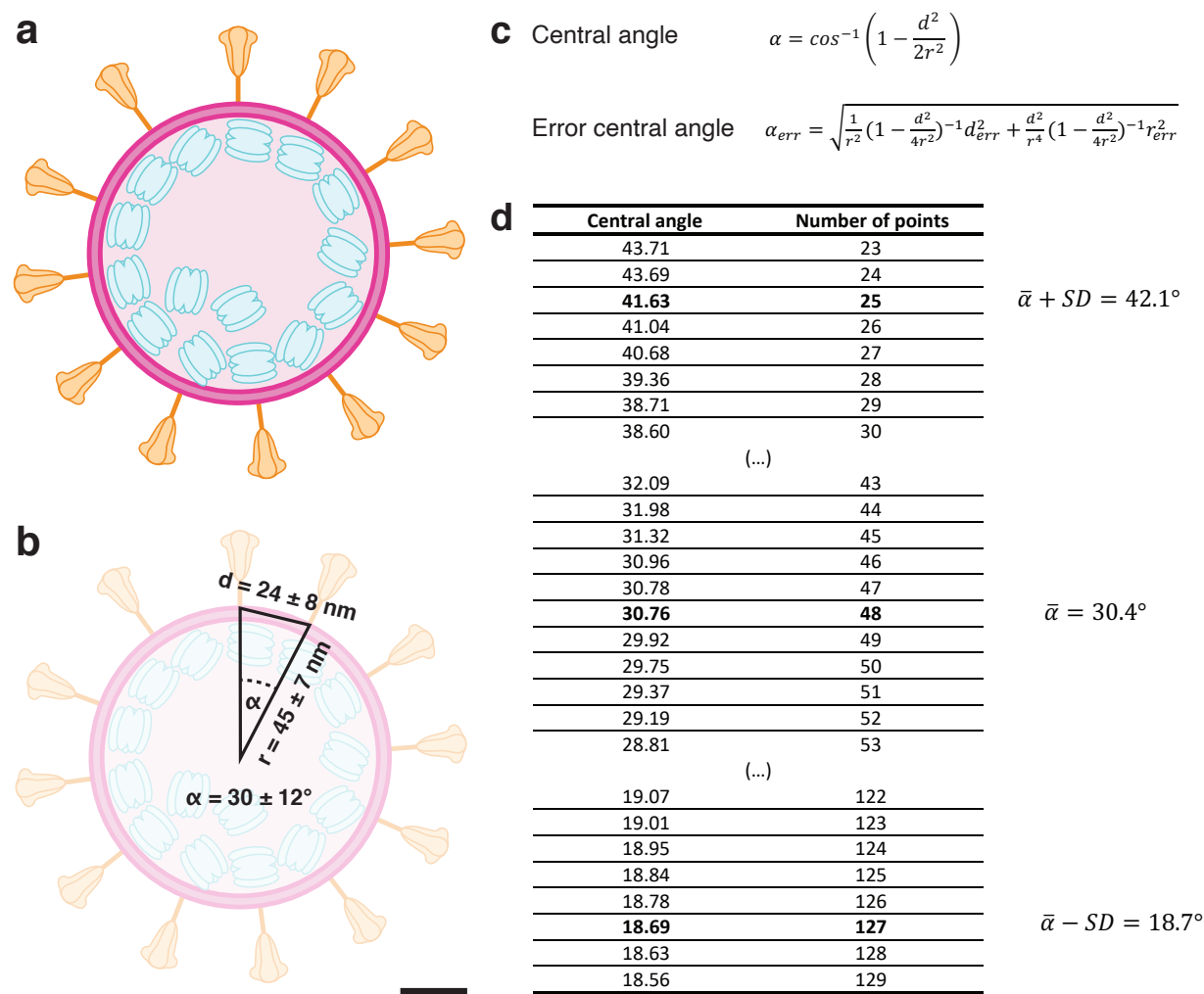


Figure S8 | Model of SARS-CoV-2 with estimation of S trimers per virion. **a, b,** Schematic model of a SARS-CoV-2 virion showing the viral envelope in magenta, vRNP in cyan and S trimers in yellow drawn to scale. The two structural transmembrane proteins M and E are not shown. The average radius $r = 45 \pm 7$ nm, average minimum distance between nearest-neighboring S trimers $d = 24 \pm 8$ nm and the corresponding average central angle $\alpha = 30 \pm 12^\circ$ are indicated in (b). **c,** Equations used for calculations of the central angle α and its error propagation. **d,** Table of estimates of the ‘Tammes Problem’ for different numbers of points on a sphere and the corresponding central angle (14). The average central angle of 30.4° corresponds closest to a conformation with 48 points on a sphere. For the limits of the confidence interval for the central angle of 18.7° and 42.1° (highlighted in bold), closest matching conformations are 25 and 127 points on a sphere, respectively. Scale bar: 20 nm.

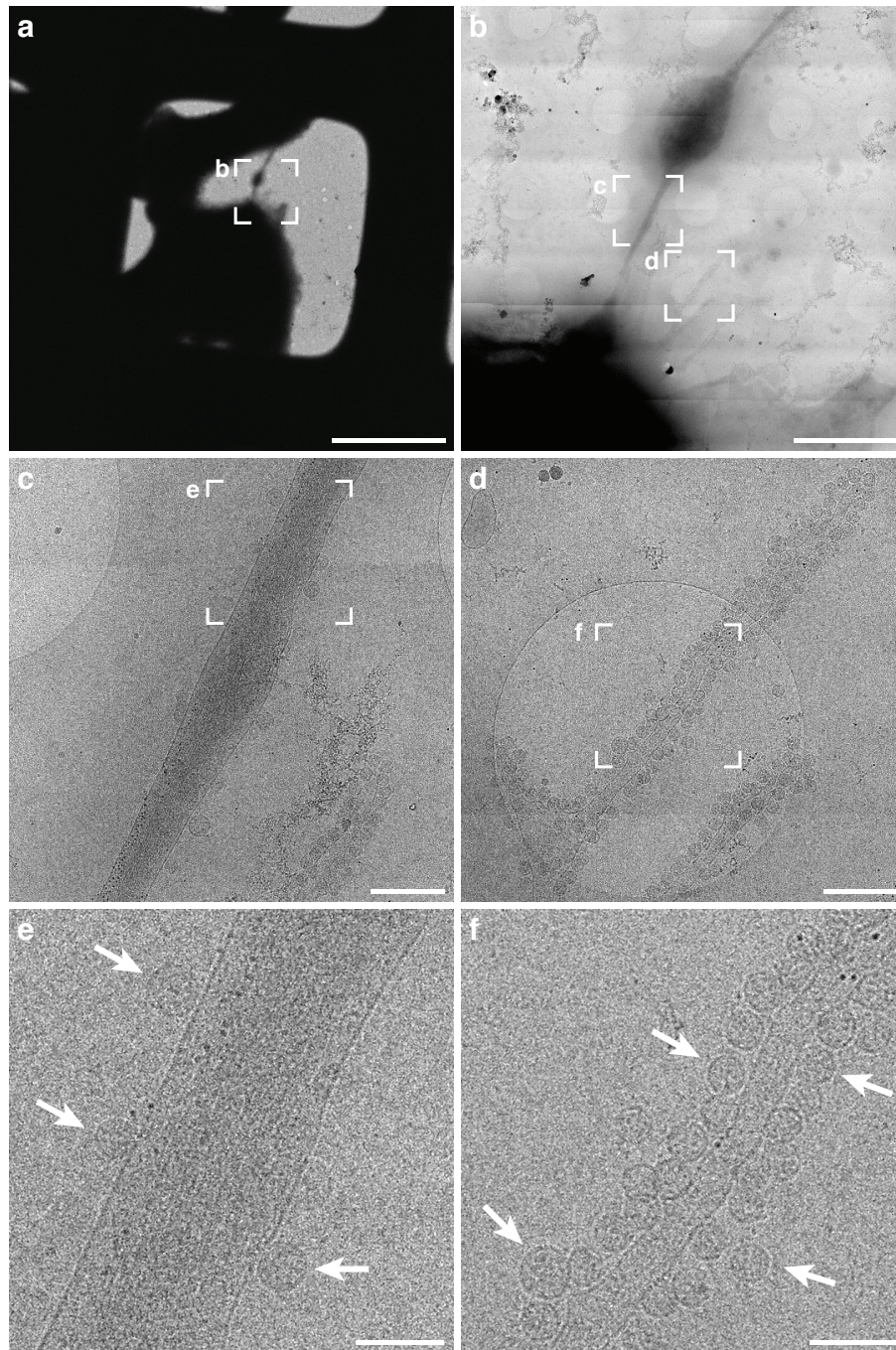


Figure S9 | Cryo-TEM of extracellular virions attached on VeroE6 cell protrusions. **a**, Low magnification cryo-TEM image of a 200 Mesh Ti grid coated with a holey carbon (Quantifoil R2/2) with infected VeroE6 cells located in a grid square. **b**, Magnified image of cell periphery denoted in (a) by a dashed square. **c**, **d**, Magnified images of cell filopodia decorated with extracellular virions denoted in (b) by dashed squares. **e**, **f**, Magnified images with individual virions (arrows) attached to the filopodia denoted in (c, d) by dashed squares. Scale bars: (a) 50 μ m, (b) 5 μ m, (c, d) 500 nm, (e, f) 200 nm.

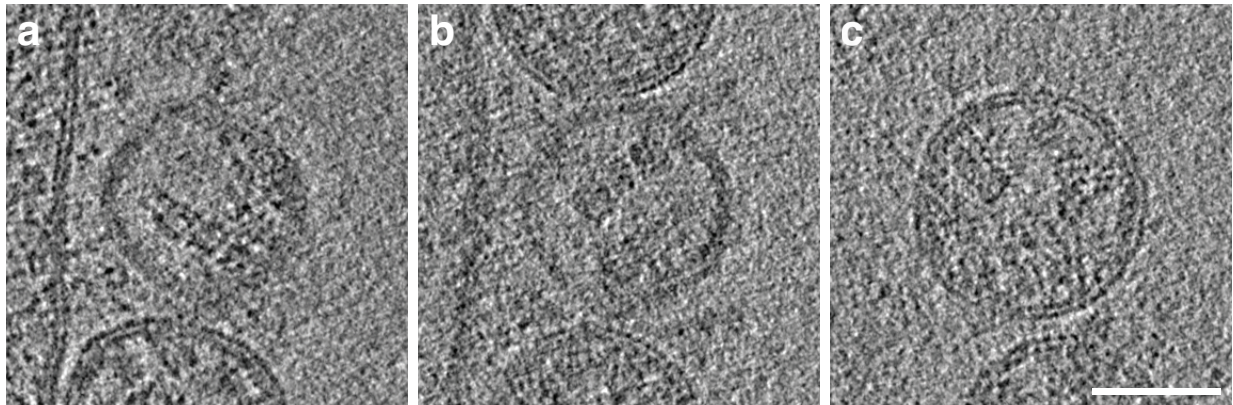


Figure S10 | Organization of vRNPs in released extracellular virions. **a–c**, Slices of tomograms of SARS-CoV-2 virions released from VeroE6 cells. Exemplarily, virions displaying linearly arranged vRNPs are shown from 3 tomograms. For better visualization, 6 slices were averaged from 3x binned and low pass filtered (2 pixel) tomograms. Scale bar: 50 nm.

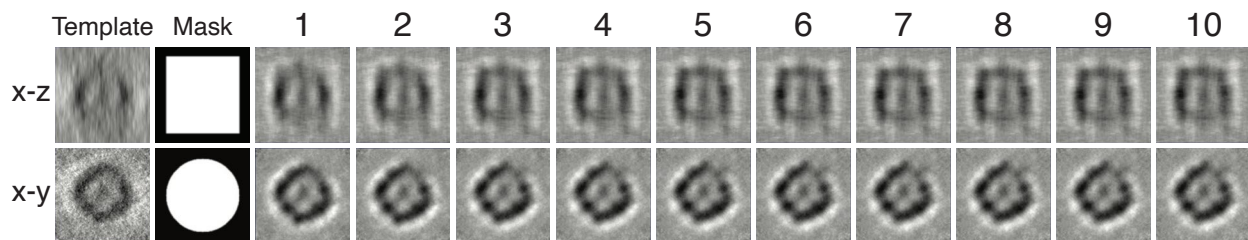


Figure S11 | Overview of vRNP subtomogram averaging. Particles ($n = 1570$) corresponding to positions of vRNPs in tomograms acquired on cryo-lamella of SARS-CoV-2 infected VeroE6 cells were cropped (168 x 168 x 168 voxels) in Dynamo using the 'general' model (7). 200 of randomly oriented particles were averaged to generate an initial template. Subsequently, particles were iteratively aligned and averaged using the template and a cylindrical mask (Movie S5).

Supplementary Materials: SARS-CoV-2 structure and replication characterized by in situ cryo-electron tomography

On-lamella cryo-ET

Infection and plunging	Cells	MOI	Infection hpi	Number of lamellae	Number of tomograms	Number of tomograms used for analysis
Sample preparation I	A459-ACE2	7	16	6	11	7
	A459-ACE2	20	16	6	10	2
	A459-ACE2	7	16	7	18	7
Sample preparation II	Calu3	5	16	12	7	3
	VeroE6	0.1	16	8	4	4
	VeroE6	0.1	16	6	8	4
	VeroE6	0.1	16	8	8	2
	A459-ACE2	20	16	7	2	1
Total				60	68	30

Whole-cell cryo-ET

Infection and plunging	Cells	MOI	Infection hpi	Number of tomograms	Number of tomograms used for analysis
Sample preparation I	A459-ACE2	20	16	5	0
Sample preparation II	A459-ACE2	20	16	3	2
	VeroE6	0.1	16	14	11
	Calu3	5	16	5	2
	VeroE6	0.1	16	13	6
Total				40	21

Table S1 | Sample preparation overview. Summary of biological replicas, number of milled lamellas, number of acquired and analyzed tomograms from each cell line used in the study.

Movie S1 | Tomogram of DMV with volume rendering and vRNA segmentation. 3D rendering of one tomogram (Fig. 1) of A549-ACE2 cells infected with SARS-CoV-2 at 16 hpi showing a DMV's outer and inner membrane (dark and light green, respectively) as well as manually segmented filaments in the DMV's core, color-coded by total filament length. The tomogram was denoised using cryo-CARE.

Movies S2 and S3 | 3D rendering of SARS-CoV-2 virion budding and assembly at the ERGIC membrane. 3D rendering from two tomograms (Fig. 3 and S6) of VeroE6 cells infected with SARS-CoV-2 at 16 hpi showing budding events at the ERGIC membrane and intracellular released virions inside the ERGIC lumen are indicated. Cellular and viral membranes are shown in green and magenta, respectively. S trimers (yellow) and vRNPs (cyan) are represented as subtomogram averages. The S and vRNP locations correspond to the location in the tomogram, vRNP orientations were randomized. A non-local means filter was applied on the tomogram, and 20 slices were averaged.

Movie S4 | 3D rendering of subtomogram average of S trimer with fitted structures. S trimer subtomogram average (yellow) and the virion envelope (magenta). Fitted structure of the S trimer ectodomain (PDB:6VXX) and the HR2 domain (PDB:2FXP) are shown in black and orange, respectively.

Movie S5 | 3D rendering of subtomogram average of vRNP. vRNP complex rotated around the long and short axis.